Diffuse large B-cell lymphoma (DLBCL) is infiltrated with activated CD8+ T-cells despite immune checkpoint signaling

Adam M. Greenbaum[1], Jonathan R. Fromm[2], Ajay K. Gopal[1,3], A. McGarry Houghton[1,4]

[1]Clinical Research Division, Fred Hutchinson Cancer Research Center, [2]Department of Laboratory Medicine, [3]Division of Medical Oncology, [4]Division of Pulmonary and Critical Care Medicine, University of Washington, Seattle, WA, USA

Ⓒ 2022 Korean Society of Hematology

Background
B-cell non-Hodgkin lymphomas (NHL) are hematologic malignancies that arise in the lymph node. Despite this, the malignant cells are not cleared by the immune cells present. The failure of anti-tumor immunity may be due to immune checkpoints such as the PD-1/PDL-1 axis, which can cause T-cell exhaustion. Unfortunately, unlike Hodgkin lymphoma, checkpoint blockade in NHL has shown limited efficacy.

Methods
We performed an extensive functional analysis of malignant and non-malignant lymph nodes using high dimensional flow cytometry. We compared follicular lymphoma (FL), diffuse large B-cell lymphoma (DLBCL), and lymph nodes harboring reactive hyperplasia (RH).

Results
We identified an expansion of CD8+PD1+ T-cells in the lymphomas relative to RH. Moreover, we demonstrate that these cells represent a mixture of activated and exhausted T-cells in FL. In contrast, these cells are nearly universally activated and functional in DLBCL. This is despite expression of counter-regulatory molecules such as PD-1, TIM-3, and CTLA-4, and the presence of regulatory T-cells.

Conclusion
These data may explain the failure of single-agent immune checkpoint inhibitors in the treatment of DLBCL. Accordingly, functional differences of CD8+ T-cells between FL and DLBCL may inform future therapeutic targeting strategies.

Key Words   Lymphoma, Immune microenvironment, Immune checkpoint inhibition

INTRODUCTION

B-cell non-Hodgkin's lymphomas (NHL) are a heterogeneous group of hematologic malignancies that account for approximately 3% of all new cancer diagnoses and cancer deaths. These tumors predominantly arise from malignant B-cells in lymph nodes, the primary site of the normal immune response. Despite this, the role that non-malignant immune cells play in the pathogenesis of NHL remains unclear. Molecular profiling in FL showed that clinical outcome could be predicted, not by the properties of the lymphoma itself, but by the properties of the immune response [1-3]. Recent work suggests that this immune response may be enhanced by the administration of immune checkpoint inhibitors that rescue poorly functional T-cells. Indeed, early stage clinical trials have already demonstrated that NHL respond to Programmed Death-1 (PD-1) inhibitors [4-8]. However, responses in DLBCL are rare [9], and even in indolent lymphomas, only a fraction of patients respond to therapy.

Several prior studies have examined the tumor microenvironment in follicular lymphoma (FL). The FL microenvironment contains cells that both support the tumors themselves and prevent an effective immune response. T-follicular helper cells (Tfh) are expanded in FL and support the malignant B-cells through production of IL-4 [10, 11]. In contrast, regulatory T-cells (Tregs) can suppress CD4+ T-cells [12, 13]. Immune checkpoints also play an important role in suppressing anti-tumor immunity. T-cells in FL ex-

pressing PD-1 [14], TIM-3 [15, 16] LAG-3 [17], TIGIT [18], and CD70 [19] all fail to activate in response to T-cell receptor engagement.

In contrast to FL, there is relatively sparse data on the immune microenvironment in diffuse large B-cell lymphoma (DLBCL). Thus, there is a need for a rigorous and comprehensive assessment of the immune microenvironment of this lymphoma subtype. Single cell immunophenotyping is a powerful tool to interrogate the immune microenvironment in lymphoma [20]. Here, we performed high dimensional flow cytometry comparing FL, DLBCL, and reactive hyperplasia (RH) to assess the hypothesis that NHL would be infiltrated by exhausted CD8$^+$ T-cells.

MATERIALS AND METHODS

Samples

Lymph node samples were obtained from core needle biopsies of pathologically confirmed RH (N=7), grade 1–3A FL (N=15), and DLBCL (N=21). These samples consisted of excess tissue from pathology specimens sent to the University of Washington Medical Center as part of routine clinical care. Samples were obtained according to a protocol approved by the Institutional Review Board (protocol 43066). The DLBCL specimens were acquired at the time of diagnosis whereas the FL specimens were a mixture of de novo and relapsed cases. All samples were processed into single cell suspensions and cryopreserved in liquid nitrogen prior to analysis.

Flow cytometry

All antibodies are from BD Biosciences unless noted otherwise. Cells were first incubated with anti-human Fcγ (2.4G2). They were then stained with one or more of the following antibodies (flurochrome, clone): CD127 FITC (fluorescein isothiocyanate, HIL-7R-M21), IFNγ FITC (MQ1-17H12), Ig lambda PE (phycoerythrin, eBiosciences, TB28-2), PD-1 PE-CF594 (EH12.1), GARP PE-CF594 (7511), CD5 PE-Cy5 (UCTH2), CTLA-4 PE-Cy5 (BNI-3), CD56 PE-Cy5.5 (CMSSB, eBiosciences), FoxP3 PE-Cy5.5 (PCH101, eBiosciences), Ig kappa PE-Cy7 (G20-193), PD-L1 PE-Cy7 (MIH1), CD4 APC (allophycocyanin, SK3), CD19 APC (1D3), PD-1 AlexaFluor 647 (E12.1), CD38 APC-R700 (HIT2), Ig kappa AlexaFluor 700 (G20-193), CXCR5 BV (Brilliant Violet) 421 (RF8B2), IL-2 BV421 (MQ1-17H12), CCR6 BV 480 (11A9), CXCR5 BV480 (RF8B2), CD33 BV570 (Biolegend, WM53), CD24 BV605 (ML5), CCR7 BV605 (3D12), CD10 BV650 (HI10a), PD-L2 BV650 (MIH18), CD25 BV711 (2A3), TIM-3 BV711 (7D3), HLA-DR BV786 (G46-6), LAG3 BV786 (T47-530), CXCR3 BUV (Brilliant Ultraviolet) 395 (1C6/CXCR3), CD45RA BUV395 (HI100), CD19 BUV496 (SJ25C1), CD4 BUV496 (SK3), CD8 BUV563 (RPA-T8), CD3 BUV661 (UCHT1), CD14 BUV737 (M5E2), CD20 BUV805 (2H7), cleaved PARP FITC (Asp214), Granzyme B PE-CF594 (GB11), Perforin BV421 (B-D48, Biolegend), CD107a BV786 (H4-A3), and Ki67 BV650 (B56). Dead cells were excluded

using Fixable Viability Dye eFluor 780 (eBiosciences). Lymphoma immunophenotype was identified per clinical flow phenotype. All flow cytometry was performed on a Fortessa X-50 or Symphony (BD Biosciences). Flow cytometry data analysis was performed using FlowJo.

Dimensional reduction

All samples were initially gated on CD14$^-$CD3$^+$ T-cells. Each sample was down-sampled and all sample files were concatenated. Samples were then analyzed using the Uniform Manifold Approximation and Projection (UMAP) [21] and Phenograph [22] algorithms to define two dimensions (UMAP_X and UMAP_Y) and computationally identify phenotypes. Analysis was performed using FlowJo plugins.

In vitro stimulation

Cells were incubated with Phorbol myristate acetate (PMA, 2 ng/mL) and ionomycin (1 µg/mL) in the presence of Brefeldin A (Golgiblock, BD Biosciences). In the degranulation assays, cells were also incubated in the presence of CD107a antibodies. For both experiments, incubation was for 5 hours in RPMI plus 10% FCS at 37°C. Cells were stained with Fc block, surface antibodies, fixed and permeabilized (eBiosciences, FoxP3 staining buffer), and stained for intracellular antigens.

Statistical analysis

Analyses were performed using GraphPad Prism. Bar graphs represent the mean and the standard error of the mean. To compare the means of different histology types, ANOVA with multiple correction analysis was performed. To compare associations between cytokines and PD-1 expression, linear regression using the least squares method was performed. To compare functional status by marker expression, ANOVA was performed with multiple correction relative to the cells expressing the fewest activation/exhaustion markers. Statistical significance was defined as $P < 0.05$.

RESULTS

Lymph node immune microenvironments differ between in NHL subtypes

We first developed a novel 22-color flow cytometry panel (Supplementary Table 1) and used it on a subset of FL, DLBCL, and RH to identify populations unique to the lymphomas. We identified 19 unique cell phenotypes through dimensional reduction using the UMAP algorithm and computationally identifying cellular subsets using Phenograph (Fig. 1A). In attempts to identify populations unique to lymph nodes containing lymphoma, we overlaid the populations present in RH (red) to identify the 6 populations enriched in the lymphomas (Fig. 1B). We then assessed the expression of CD45RA, FoxP3, CXCR5, PD-1, and TIM-3. As expected, RH was enriched in CD45RA$^+$ cells consistent with a naïve phenotype (Fig. 1C). Population 1 was enriched for CD4$^+$
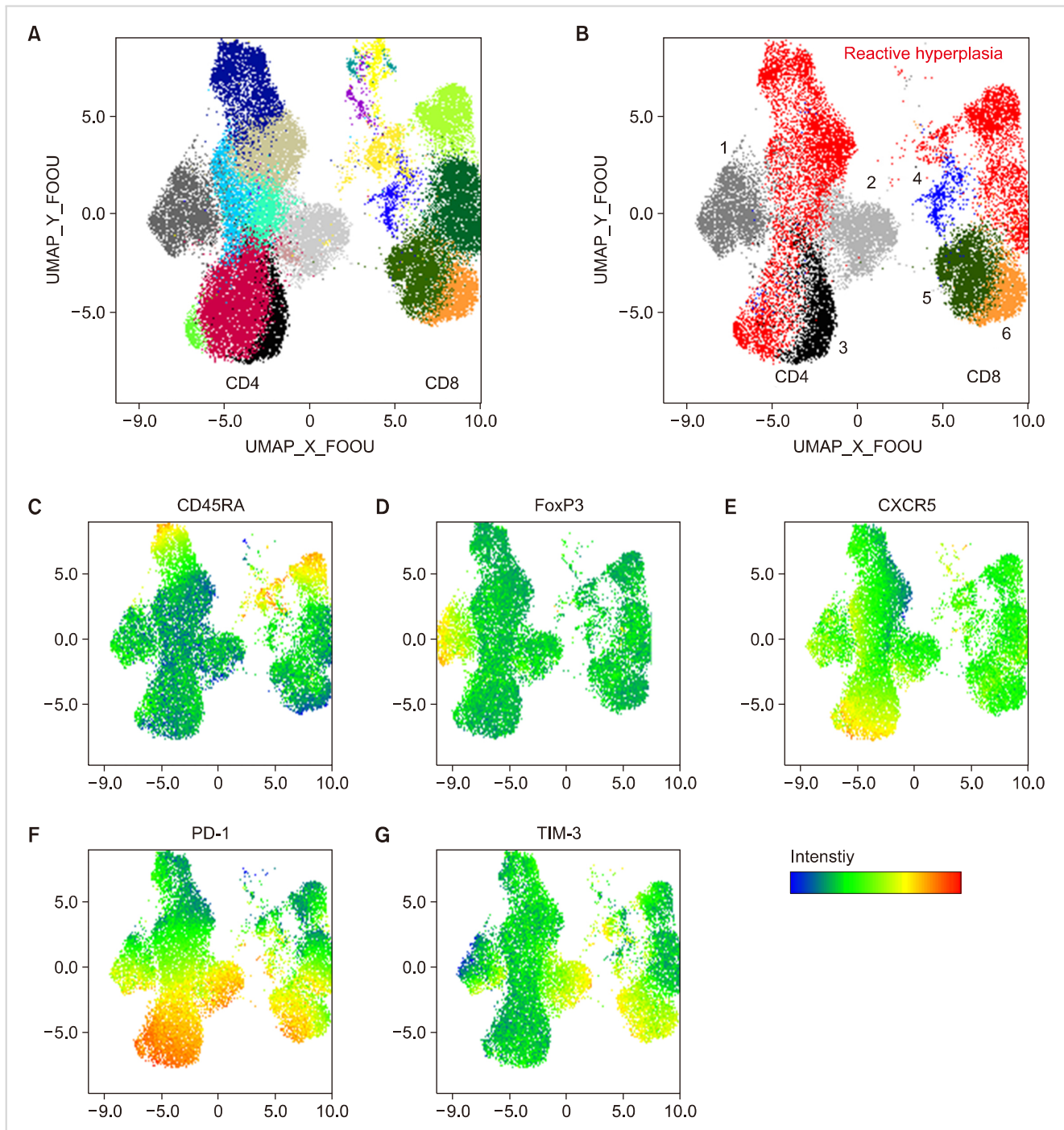
Fig. 1. Dimensional reduction of T-cells using UMAP algorithm. **(A)** U-MAP plot of T-cells generated from combined data from RH, FL, and DLBCL. Each color represents an identified population using the PhenoGraph algorithm. **(B)** Overlay of reactive hyperplasia (red) on to U-MAP plot. Numbers represent populations not present RH. **(C–G)** Heat maps showing expression of CD45RA, FoxP3, CXCR5, PD-1, and TIM-3. Histologies were FL (N=7), DLBCL (N=6), and RH (N=2). DLBCL subtypes included 4 GCB type, 1 ABC type, and one unknown.

FoxP3+ regulatory T-cells (Fig. 1B, D). Population 2 was enriched for CD4+ PD1+ TIM3+ T-cells (Fig. 1B, F, G). Population 3 consisted with CD4+ CXCR5+ PD1+ T-follicular helper cells (Fig. 1B, E, F). Population 4 is of unclear cellular identity and lacked most markers in this panel except TIM-3. Populations 5 and 6 were enriched for CD8+PD1+TIM3+ T-cells that expressed minimal differences in PD-L1 of un-

clear significance (Fig. 1B, F, G, not shown).

We next performed a separate novel 22-color flow cytometry panel in much larger cohort of lymphomas (Supplementary Table 1). This panel was designed to further characterize the T-cells of interest (Table 1). We confirmed a trend towards expansion of Tfh in FL and a near absence of Tfh in DLBCL consistent with prior reports (Fig. 2A)

Table 1. Populations assessed using flow cytometry.

Cell type	Subpopulation	Immunophenotype
Myeloid	Monocyte	CD33$^+$ CD14$^+$ HLA-DR^{hi}
	Monocytic myeloid derived suppressor cell	CD33$^+$ CD14$^+$ HLA-DRlo
B-cell CD19$^+$ CD20$^+$	Memory	CD24$^+$ CD38$^-$
	Mature	CD24$^+$ CD38$^+$
	B10 regulatory	CD24^{hi} CD38^{hi}
Natural killer	NK	CD3$^-$ CD56$^+$
	NK T-cell	CD3$^+$ CD56$^+$
CD4 T-cells CD3$^+$ CD4$^+$	Regulatory (Treg)	CD127^{low} CD25$^+$ CXCR5$^-$
	PD-1$^-$	CXCR5$^-$ PD-1$^-$
	PD-1^{int}	CXCR5$^-$ PD-1^{int}
	Th1	CXCR5$^-$ CCR6$^-$ CXCR3$^+$
	Th2	CXCR5$^-$ CCR6$^-$ CXCR3$^-$
	Th17	CXCR5$^-$ CCR6$^+$ CXCR3-
Follicular T-cells CD4$^+$ CXCR5$^+$ PD-1^{hi}	Follicular helper (Tfh), CD10$^+$	CD10$^+$
	Follicular helper, CD10$^-$	CD10$^-$
	Follicular regulatory (Tfr)	CD127^{low} CD25$^+$
	Tfh-Th1	CCR6$^-$ CXCR3$^+$
	Tfh-Th2	CCR6$^-$ CXCR3$^-$
	Tfh-Th17	CCR6$^+$ CXCR3$^-$
CD8 T-cells CD3$^+$ CD8$^+$	Regulatory (Treg)	CD127^{low} CD25$^+$ CXCR5$^-$
	PD-1$^-$	CXCR5$^-$ PD-1$^-$
	PD-1$^+$	CXCR5$^-$ PD-1$^+$
	CXCR5$^+$	CXCR5$^+$
Dendritic cell	Myeloid dendritic cell	CD14$^-$ CD33$^+$ HLA-DR$^+$
	Pre-dendritic cells	CD14$^+$ CD33- HLA-DR$^+$

Shown are the cell populations analyzed, their subpopulations, and their immunophenotypes.

[11]. We also confirmed an expansion of Tregs in FL (Fig. 2B). Surprisingly, these Tregs expressed similar levels of the activation marker GARP [23] to RH, suggesting that these Tregs are largely inactive (data not shown). Although we initially observed a population of CD3$^-$TIM3$^+$ cells in the clustering analysis, CD56$^+$CD3$^-$NK cells were not changed in numbers in the validation cohort (Fig. 2C). Notably, there was no overall expansion of CD4$^+$PD-1$^-$ or CD4$^+$PD-1^{int} cells. In contrast, there was a strong trend towards expansion of CD4$^+$PD-1^{int} cells that expressed TIM3, although this was not statistically significant (Fig. 2D–F). We observed a similar finding in CD8$^+$ cells with no expansion in CD8$^+$ PD-1$^-$ cells but a stronger expansion of CD8$^+$ PD-1$^+$ cells most prominently in DLBCL. Again, this was primarily in the CD8$^+$PD-1$^+$TIM-3$^+$ population, with these double-positive cells representing on average 20% of all infiltrating immune cells (Fig. 2H, I). Within the DLBCL cohort, there were few differences between activated B-cell type (ABC) and germinal center B-cell (GCB) type, although there were statistically more CD4$^+$ PD1^{int} T-cells in the ABC subtype (Supplementary Fig. 1).

CD8$^+$ T-cells expressing activation/exhaustion markers are effector T-cells with retained ability to produce IFNγ

Given the statistically significant expansion of CD8$^+$ PD-1$^+$ T-cells but equivocal changes in the CD4$^+$ cellular compartment, we focused further studies on CD8$^+$ cells. We charac-

terized the CD8$^+$ T-cells expressing the activation/exhaustion markers for their effector/memory phenotype. While ~50% of CD8$^+$ T-cells were in a naïve state in RH, these cells were heavily skewed towards a memory phenotype in NHL, suggesting prior antigen exposure. This population was comprised of a mixture of both central and effector memory cells (Fig. 3A). This suggests that the CD8$^+$ T-cells in NHL are antigen experienced. We next asked whether PD-1 could be a consistent marker for antigen exposure. Indeed, PD-1$^+$CD8$^+$ cells are skewed towards the memory phenotype, although this is unchanged upon further expression of TIM-3 (Fig. 3B).

We examined whether these antigen experienced CD8$^+$ T-cells remained functional in terms of cytokine production upon stimulation with PMA and ionomycin. Minimal amounts of these cytokines were observed without stimulation (data not shown). Compared to reactive lymph nodes, bulk CD8$^+$ T-cells from lymphoma specimens produced higher levels of interferon gamma (IFNγ) (Fig. 3C). There was no difference in production of IL-2 (not shown). Higher IFNγ production was seen across naive, central memory, effector memory, and TEMRA subsets suggesting that the phenotype in bulk CD8$^+$ T-cells was not due to skewing away from naive T-cells (Fig. 3D).

Given that PD-1 is a marker for antigen exposure, we suspected that PD-1 could be a reliable marker for T-cell activation or exhaustion. In DLBCL, PD-1 expression pos-
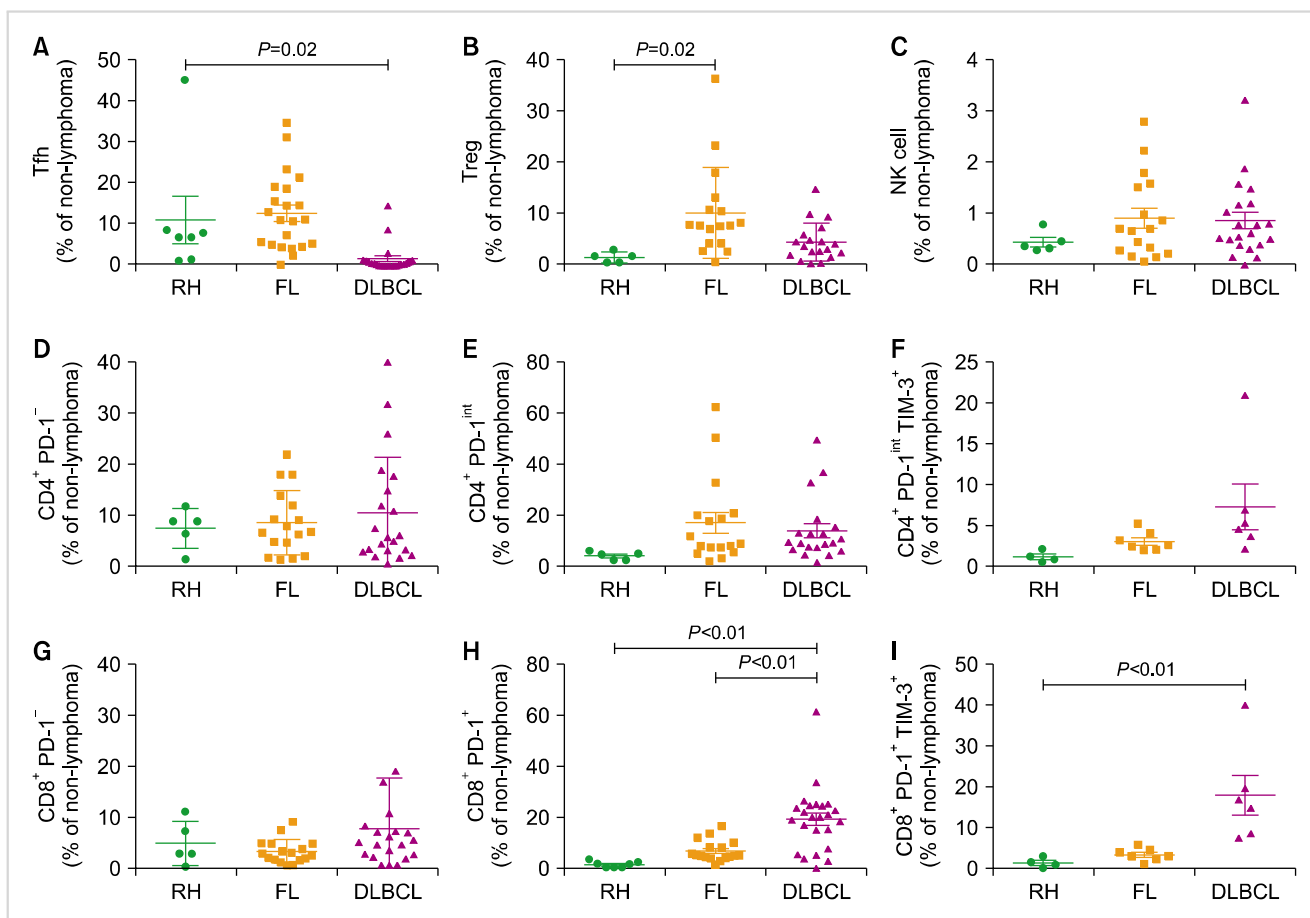
Fig. 2. Populations enriched in each histology. **(A)** Tfh, **(B)** Treg, **(C)** NK cells, **(D)** CD4$^+$ PD-1$^-$, **(E)** CD4$^+$ PD-1^{int}, **(F)** CD4$^+$ PD-1^{int} TIM-3$^+$, **(G)** CD8$^+$ PD-1$^-$, **(H)** CD8$^+$ PD-1$^+$, **(I)** CD8$^+$ PD-1$^+$ TIM-3$^+$. Graphs represent a separate cohort of patients from **Fig. 1** except panels F and I. Histologies for new cohort were RH (N=4), FL (N=16), DLBCL (N=20). *P*-values as indicated.

itively correlated with IFNγ production (Fig. 3E). PD-1 expression also weakly trended with IL-2 production (Fig. 3F), suggesting that PD-1 serves an activation marker in this histology. However, these correlations did not appear to hold for FL, suggesting that PD-1 serves as both an activation and exhaustion marker in that setting. To further explore this, we looked at T-cell exhaustion based on expression of other exhaustion/activation markers including PD-1, TIM-3, LAG-3, and CTLA-4 (Fig. 3G, H). Since LAG-3 was expressed at low levels on CD8$^+$ T-cells, this could not be assessed in LAG-3$^+$ populations (data not shown). In the conventional model, progressive expression of these molecules is associated with increasing exhaustion [24]. Surprisingly, progressive acquisition of PD-1, TIM-3, and CTLA-4 was associated with increased CD8$^+$ T-cell activation with 70–80% of the triple positive cells producing IFNγ. In contrast, we observed the opposite trend in IL-2. Notably, this trend was not seen in RH, with triple positives either producing the same amount of IL-2 or increasing amounts (Fig. 3H). Additionally, PD-1$^+$ cells also down-regulate IL-7Rα (CD127) which is often seen in activated cells (data not shown). This suggests that CD8$^+$ PD-1$^+$ TIM-3$^+$ CTLA-4$^+$ T-cells are highly activated and have a phenotype similar

to effector T-cells, which produce IFNγ, downregulate IL-7Rα, and decrease their production of IL-2 [25]. In sum, NHL are characterized by infiltration of highly activated CD8$^+$ effector and memory T-cells. While these activated cells are present to some degree in FL, they represent the majority of all infiltrating T-cells in DLBCL.

CD8$^+$ T-cells expressing activation/exhaustion markers retain cytotoxic activity with no change of cell cycling or apoptosis

We next examined other markers of T-cell cytotoxicity, as cytokine production can be disjointed from T-cell cytotoxicity [26]. Given the strong activation phenotype seen in DLBCL, we limited our analysis to this histology. As CD8$^+$ T-cells increasingly express counter-regulatory receptors, they show signs of increasing cytotoxic potential. Contrary to the expected immunophenotype of exhausted cells, they express intracellular perforin and granzyme. They also maintain their ability to degranulate in response to stimulation as assessed by staining for cell surface CD107a, a protein present in the membranes of cytotoxic granules that is only present on the cell surface upon degranulation (Fig. 4A, B) [27].
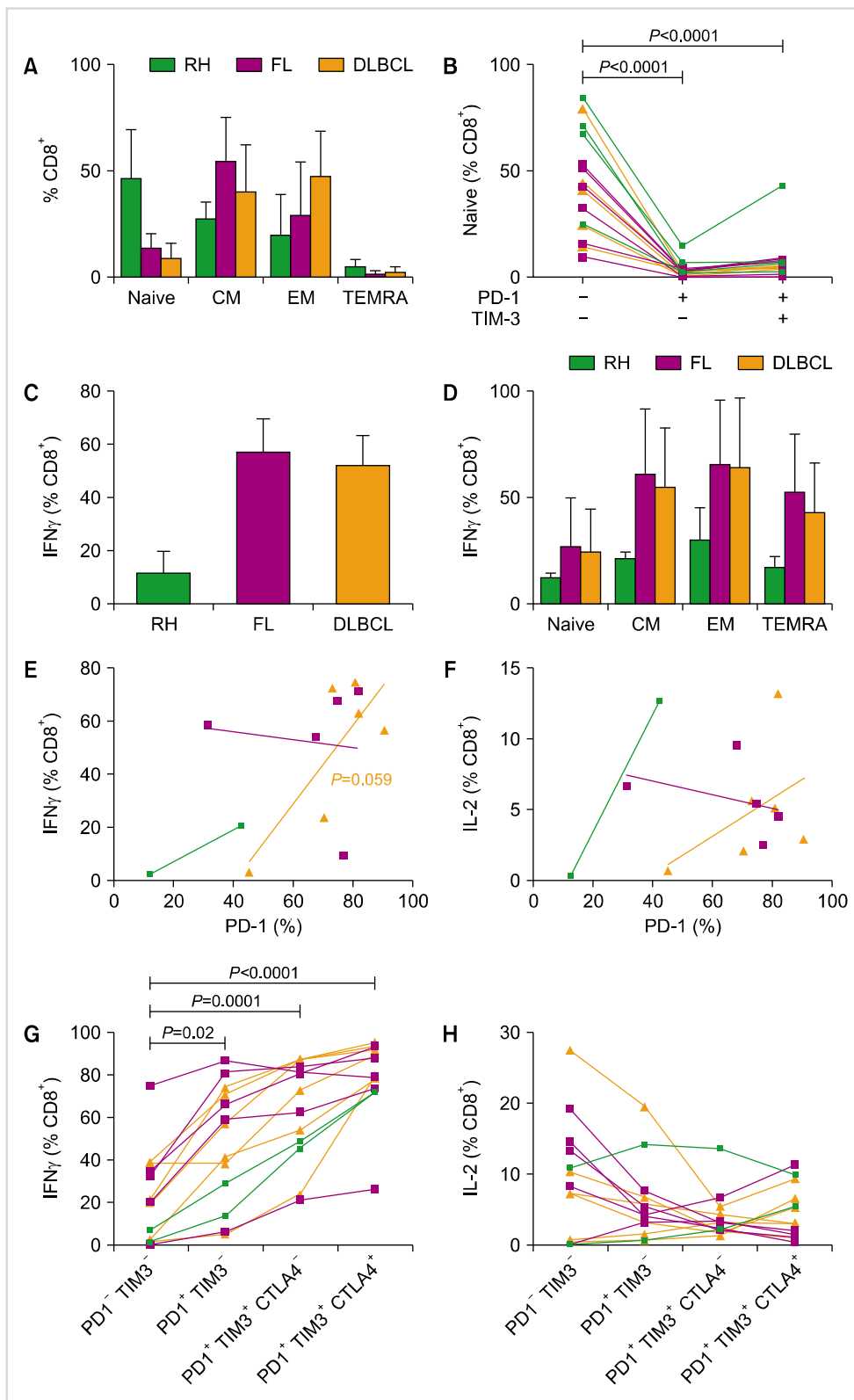
Fig. 3. Functional characterization of CD8$^+$ cells. The percentage of (**A**) naïve/central memory (CM)/ effector memory (EM) T-cells by each histology and (**B**) by expression of PD-1 and TIM-3 expression. (**C**) Percent of total CD8$^+$ T-cells that produce IFNγ. (**D**) IFNγ production by histology and memory subset. (**E, F**) Linear regression of CD8$^+$ cells producing IFNγ and IL-2 versus the percentage of cells expressing PD-1. (**G**) IFNγ and (**H**) IL-2 production by CD8$^+$ T-cells by expression of PD-1, TIM-3, and CTLA-4. Histologies were RH (N=2), FL (N=5), DLBCL (N=6). *P*-values as indicated.

One potential explanation is that these cells have lower proliferative potential with an increased sensitivity to apoptosis, as seen in CD127$^-$CD8$^+$ cells in HIV. However, this populations does not display decreased proliferation or increased apoptosis in DLBCL. Together, these data suggest that the CD8$^+$ T-cells in DLBCL are highly functional with no defects in proliferation or cell survival (Fig. 4C, D).
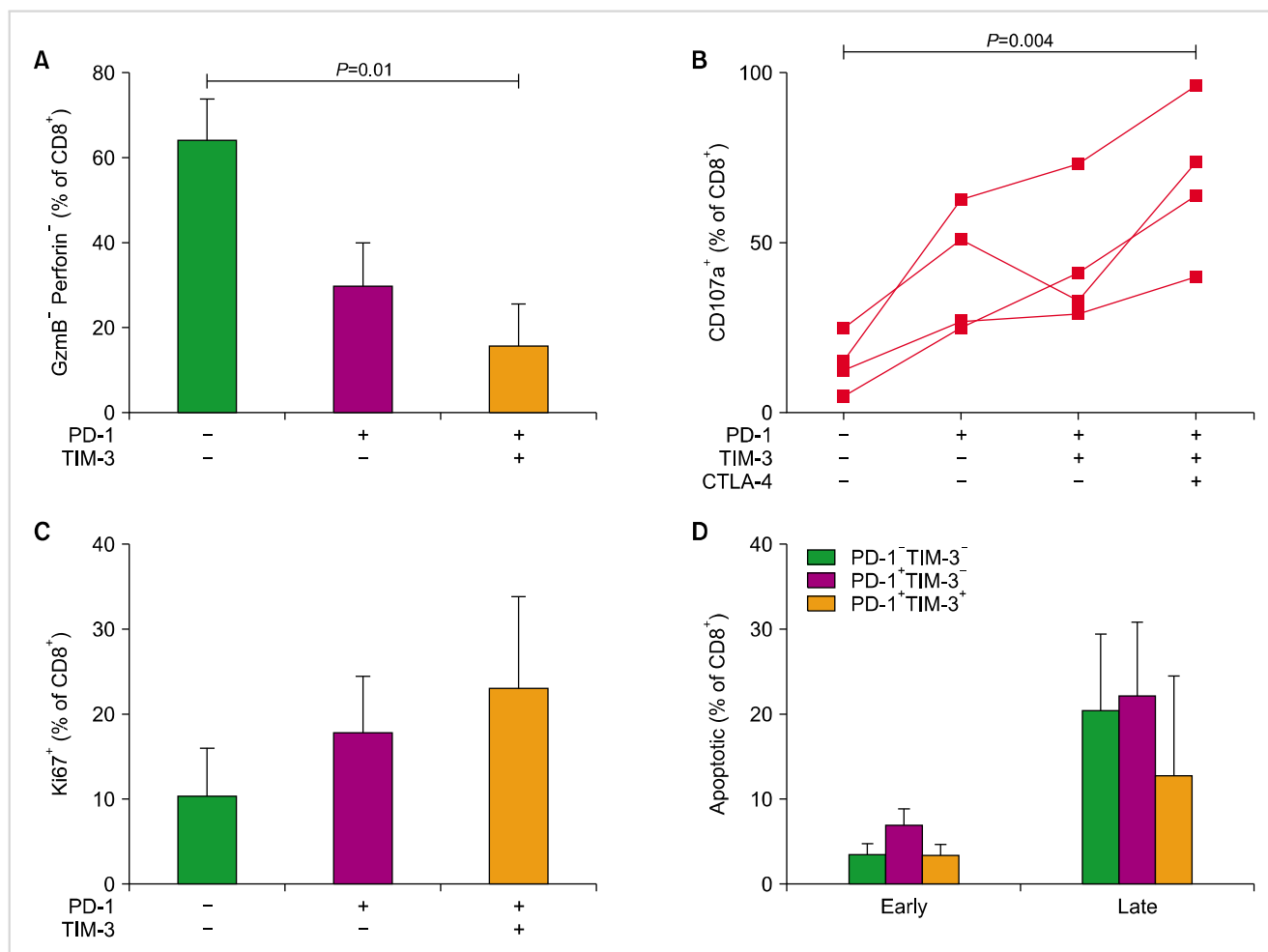
Fig. 4. Cytotoxicity, cell cycling, and apoptosis in DLBCL. **(A)** The percentage of CD8⁺ T-cells lacking both granzyme B and perforin by PD-1 and TIM-3 expression (N=4). **(B)** The percentage of CD8⁺ T-cells that degranulate in response to PMA/ionomycin by PD-1, TIM-3, and CTLA-4 expression (N=4). **(C)** The percentage of CD8⁺ T-cells that are actively cycling by PD-1 and TIM-3 expression (N=4). **(D)** Percentage of CD8⁺ T-cells that are undergoing apoptosis by PD-1 and TIM-3 expression. Early apoptosis is defined as cleaved PARP⁺ viability dye-, and late apoptosis as cleaved PARP⁺ viability dye⁺ (N=4). *P*-values as indicated.

DISCUSSION

Immune checkpoint inhibitors (ICI), including anti-PD-1 antibodies, have revolutionized the therapeutic landscape of oncology, which likely exert their effect by reversing T-cell exhaustion. Unfortunately, studies of these drugs in NHL have largely been disappointing, with response rates in the single digits [4, 6, 7]. Whether the PD-1/PD-L1 axis mediates the infrequent responses to treatment remains unclear. In a trial of single agent nivolumab in relapsed DLBCL, elevated PD-L1 expression was present in only 9% of lymphomas, but the majority of responding patients did not have PD-L1 expression in their tumors [9]. Similarly, in a trial combining nivolumab with ibrutinib in relapsed DLBCL, elevated PD-L1 expression was again rare but was associated with complete response but not overall response [9]. In contrast, a recent study from our center of untreated DLBCL demonstrated that 83% of the specimens expressed PD-L1, and that PD-L1 was associated with excellent out-comes when the patients were treated with pembrolizumab+ R-CHOP [28]. Results of ICI in relapsed/refractory FL have been disappointing with an overall response rate of just 4% to singe agent nivolumab [29], despite more encouraging initial data [30].

Here, we demonstrate that CD8⁺ T-cells infiltrating DLBCL are highly activated and lack an exhausted phenotype. We show that the expression of counter-regulatory receptors such as PD-1, TIM-3, or CTLA-4 also does not mark T-cell exhaustion. Similar findings were reported in an independent study in DLBCL just last year [31]. This runs contrary to the classical exhaustion model seen in viral infections. In chronic viral infection, PD-1 is rapidly upregulated upon antigen stimulation and T-cell activation [32], but constitutive expression due to chronic antigen stimulation can result in T-cell exhaustion [33]. However, some studies have questioned whether this biology holds true in other settings. In both healthy human lymphocytes and tumor infiltrating lymphocytes, CD8⁺PD-1⁺ T-cells have similar capacity to produce inflammatory cytokines such as IFNγ, IL-2, and

TNFα compared to PD-1⁻ cells [34, 35]. Similarly, in melanoma patients immunized against the melanoma antigen MART1, antigen-specific T-cells retained their ability to secrete IFNγ, produce granzyme B, and degranulate regardless of PD-1 expression [34]. Acquisition of other immune checkpoint receptors is also not synonymous with exhaustion. In chronic viral infection, co-expression of PD-1 and TIM-3 represents the most functionally exhausted T-cells [36, 37]. In contrast, circulating tumor-specific T-cells in melanoma patients maintain their function despite expressing high levels of PD-1, TIM-3, and CTLA-4 [38].

The biology can also vary depending on the organ microenvironment. In colorectal cancer, CD8$^+$PD-1$^+$ T-cells have different phenotypes in the tumor and lymph nodes. While PD-1 defines exhausted T-cells in the tumor, PD-1$^+$ cells in the draining lymph nodes retain their functional capacity [39]. In CLL, circulating PD-1$^+$CD8$^+$ T-cells retain their ability to produce cytokines. In contrast to the phenotype we observe in DLBCL, these CD8$^+$ T-cells have defective cytotoxicity [26]. Together, these data suggest that the function of PD-1$^+$ T-cells may largely depend on the immunologic milieu.

With the presence of highly activated and functional T-cells in NHL, it remains unclear why T-cells cannot eradicate the tumor. One possibility is the defect in production of IL-2, although the role of IL-2 in CD8$^+$ T-cells is unclear. Some have described CD8$^+$ T-cells with reduced IL-2 production capacity as highly cytotoxic effector cells [25]. Others have described two populations of CD8$^+$ T-cells during the effector phase of viral infection: those that co-produce IFNγ and IL-2, and those that only produce IFNγ. During the effector phase, the IL-2 producing T-cells have increased survival and potential to become memory cells. However, the IL-2 non-producing cells can also develop into memory cells with equivalent response upon antigen re-challenge [40]. Additionally, lymphomas may be infiltrated with regulatory T-cells that can suppress other aspects of T-cell function. Indeed, we observed a slightly increased number of Tregs in NHL, but a minority were activated. Another possibility is that there are not sufficient tumor antigens to stimulate the T-cells. However, DLBCL has one of the highest tumor mutational burdens among cancers, comparable to other cancers that respond robustly to checkpoint inhibitors such as melanoma or non-small cell lung cancer [41]. Another possible explanation is that these antigens are not presented to the T-cells. Indeed, approximately half of all DLBCLs lose their expression of HLA class I [42]. Additionally, we observed that dendritic cells—which some suggest are a major presenter of tumor antigens—were extremely rare (data not shown). Even if antigen presentation is occurring, the large T-cell activation may represent the "bystander" effect, in which non-tumor-reactive T-cells expand in response to an inflammatory environment caused by the tumor [43]. The tumors may not be infiltrated with the T-cells. Indeed, in our cohort, there was tremendous variation in T-cell numbers. In DLBCL, CD8$^+$ PD-1$^+$ T-cells represented anywhere between 0.3% and 31% of all cells

with a mean of 10%. Finally, the T-cells may have defects in formation of the immunologic synapse and thus lose killing ability. This has been described in FL [43], although it remains controversial [15]. It has also been described in a very small subset of DLBCL, although it appears to be primarily for DLBCL previously transformed from FL which may exhibit different biology than de novo DLBCL [44].

There are some limitations to our study that are worthy of discussion. Due to the limited sample size, it possible that the samples we analyzed are not representative of DLBCL as a whole. Nevertheless, these data suggest that there is a subset of DLBCL patients who lack hallmarks of exhaustion. Although we assessed T-cell killing ability by monitoring cytokine production, granule production, and degranulation, we did not directly test T-cell cytotoxicity in killing assays. It is also unclear whether immune checkpoint inhibition can alter the immune microenvironment to restore T-cell killing. We are currently examining this in two clinical trials of immune checkpoint inhibitors. It is also unclear what effect the degree of T-cell activation has upon clinical outcome. Because of our limited sample size—nearly all of which contain highly activated T-cells—we could not assess this. However, the presence of PD-1$^+$ tumor infiltrating lymphocytes is positively correlated with a better prognosis in DLBCL [45-47] suggesting that CD8$^+$PD-1$^+$ T-cells may help clear the tumor in certain circumstances. Finally, although CD4$^+$ T-cells play an important part of anti-tumor immunity, we did not examine them in this study because we could not reliably identify changes relative to reactive lymph nodes using our assays.

Notably, our results run contrary to others that suggest that CD8$^+$PD-1$^+$ T-cells have defective production of cytokines such as IFNγ [48]. However, this discrepancy may be explained by important methodological differences. In the prior study, cells were stimulated through the T-cell receptor with anti-CD3/CD28 beads which results in production of modest levels of IFNγ. In our study, the T-cell receptor was bypassed through use of PMA and ionomycin which is a significantly stronger stimulus that favors production of IFNγ. Additionally, in the prior study, cells were stimulated for 6 hours. Cytokine production upon T-cell stimulation through CD3/CD28 is quite modest at 6 hours and does not peak until 24 hours. In contrast, PMA and ionomycin produces peak production after approximately 6 hours [49]. This suggests that PD-1$^+$ T-cells may show decreased cytokine production upon relatively short and weak T-cell signaling, but this can be bypassed by a stronger stimulus. In other words, expression of immune checkpoint receptors may represent T-cells that retain the capacity for rapid and robust activation.

In sum, DLBCL is characterized by the infiltration of highly functional CD8$^+$ T-cells that lack the major hallmarks of exhaustion despite expression of counter-regulatory receptors. This biology may explain the failure of PD-1 inhibitors in this disease, as they require PD-1 mediated exhaustion in order to exert their effect. However, given rare patients who enjoy durable responses to PD-1 inhibitors,

there may be a subset of patients that show a true exhaustion phenotype. Assessing CD8+ T-cell function may help identify which patients may benefit from these drugs.

Authors' Disclosures of Potential Conflicts of Interest

No potential conflicts of interest relevant to this article were reported.

REFERENCES

1. Dave SS, Wright G, Tan B, et al. Prediction of survival in follicular lymphoma based on molecular features of tumor-infiltrating immune cells. N Engl J Med 2004;351:2159-69.
2. Alizadeh AA, Gentles AJ, Alencar AJ, et al. Prediction of survival in diffuse large B-cell lymphoma based on the expression of 2 genes reflecting tumor and microenvironment. Blood 2011;118:1350-8.
3. Rosenwald A, Wright G, Chan WC, et al. The use of molecular profiling to predict survival after chemotherapy for diffuse large-B-cell lymphoma. N Engl J Med 2002;346:1937-47.
4. Lesokhin AM, Ansell SM, Armand P, et al. Nivolumab in patients with relapsed or refractory hematologic malignancy: preliminary results of a phase Ib study. J Clin Oncol 2016;34:2698-704.
5. Westin JR, Chu F, Zhang M, et al. Safety and activity of PD1 blockade by pidilizumab in combination with rituximab in patients with relapsed follicular lymphoma: a single group, open-label, phase 2 trial. Lancet Oncol 2014;15:69-77.
6. Ding W, Laplant B, Witzig TE, et al. PD-1 blockade with pembrolizumab in relapsed low grade non-Hodgkin lymphoma. Blood (ASH Annual Meeting Abstracts) 2017;130(Suppl):4055.
7. Nastoupil LJ, Westin JR, Fowler NH, et al. Response rates with pembrolizumab in combination with rituximab in patients with relapsed follicular lymphoma: interim results of an on open-label, phase II study. J Clin Oncol (ASCO Annual Meeting Abstracts) 2017;35(Suppl):7519.
8. Younes A, Brody J, Carpio C, et al. Safety and activity of ibrutinib in combination with nivolumab in patients with relapsed non-Hodgkin lymphoma or chronic lymphocytic leukaemia: a phase 1/2a study. Lancet Haematol 2019;6:e67-78.
9. Ansell SM, Minnema MC, Johnson P, et al. Nivolumab for relapsed/refractory diffuse large B-cell lymphoma in patients ineligible for or having failed autologous transplantation: a single-arm, phase II study. J Clin Oncol 2019;37:481-9.
10. Amé-Thomas P, Hoeller S, Artchounin C, et al. CD10 delineates a subset of human IL-4 producing follicular helper T cells involved in the survival of follicular lymphoma B cells. Blood 2015;125: 2381-5.
11. Amé-Thomas P, Le Priol J, Yssel H, et al. Characterization of intratumoral follicular helper T cells in follicular lymphoma: role in the survival of malignant B cells. Leukemia 2012;26:1053-63.
12. Yang ZZ, Novak AJ, Stenson MJ, Witzig TE, Ansell SM. Intratumoral CD4+CD25+ regulatory T-cell-mediated suppression of infiltrating CD4+ T cells in B-cell non-Hodgkin lymphoma. Blood 2006;107:3639-46.
13. Mittal S, Marshall NA, Duncan L, Culligan DJ, Barker RN, Vickers MA. Local and systemic induction of CD4+CD25+ regulatory T-cell population by non-Hodgkin lymphoma. Blood 2008;111: 5359-70.
14. Myklebust JH, Irish JM, Brody J, et al. High PD-1 expression and suppressed cytokine signaling distinguish T cells infiltrating follicular lymphoma tumors from peripheral T cells. Blood 2013; 121:1367-76.
15. Gravelle P, Do C, Franchet C, et al. Impaired functional responses in follicular lymphoma CD8+TIM-3+ T lymphocytes following TCR engagement. Oncoimmunology 2016;5:e1224044.
16. Yang ZZ, Grote DM, Ziesmer SC, et al. IL-12 upregulates TIM-3 expression and induces T cell exhaustion in patients with follicular B cell non-Hodgkin lymphoma. J Clin Invest 2012;122:1271-82.
17. Yang ZZ, Kim HJ, Villasboas JC, et al. Expression of LAG-3 defines exhaustion of intratumoral PD-1+ T cells and correlates with poor outcome in follicular lymphoma. Oncotarget 2017;8:61425-39.
18. Josefsson SE, Huse K, Kolstad A, et al. T cells expressing checkpoint receptor TIGIT are enriched in follicular lymphoma tumors and characterized by reversible suppression of T-cell receptor signaling. Clin Cancer Res 2018;24:870-81.
19. Yang ZZ, Grote DM, Xiu B, et al. TGF-β upregulates CD70 expression and induces exhaustion of effector memory T cells in B-cell non-Hodgkin's lymphoma. Leukemia 2014;28:1872-84.
20. Cader FZ, Schackmann RCJ, Hu X, et al. Mass cytometry of Hodgkin lymphoma reveals a CD4+ regulatory T-cell-rich and exhausted T-effector microenvironment. Blood 2018;132:825-36.
21. McInnes L, Healy J, Melville J. UMAP: Uniform Manifold Approximation and Projection for Dimension Reduction. arXiv: 1802.03426, 2018. (Accessed February 8, 2019, at https://arxiv.org/pdf/1802.03426.pdf).
22. Levine JH, Simonds EF, Bendall SC, et al. Data-driven phenotypic dissection of AML reveals progenitor-like cells that correlate with prognosis. Cell 2015;162:184-97.
23. Wang R, Wan Q, Kozhaya L, Fujii H, Unutmaz D. Identification of a regulatory T cell specific cell surface molecule that mediates suppressive signals and induces Foxp3 expression. PLoS One 2008;3:e2705.
24. McMahan RH, Golden-Mason L, Nishimura MI, et al. Tim-3 expression on PD-1+ HCV-specific human CTLs is associated with viral persistence, and its blockade restores hepatocyte-directed in vitro cytotoxicity. J Clin Invest 2010;120:4546-57.
25. Paiardini M, Cervasi B, Albrecht H, et al. Loss of CD127 expression defines an expansion of effector CD8+ T cells in HIV-infected individuals. J Immunol 2005;174:2900-9.
26. Riches JC, Davies JK, McClanahan F, et al. T cells from CLL patients exhibit features of T-cell exhaustion but retain capacity for cytokine production. Blood 2013;121:1612-21.
27. Betts MR, Brenchley JM, Price DA, et al. Sensitive and viable

identification of antigen-specific CD8+ T cells by a flow cytometric assay for degranulation. J Immunol Methods 2003;281:65-78.

28. Smith SD, Till BG, Shadman MS, et al. Pembrolizumab with R-CHOP in previously untreated diffuse large B-cell lymphoma: potential for biomarker driven therapy. Br J Haematol 2020;189:1119-26.

29. Armand P, Janssens A, Gritti G, et al. Efficacy and safety results from CheckMate 140, a phase 2 study of nivolumab for relapsed/refractory follicular lymphoma. Blood 2021;137:637-45.

30. Nastoupil L, Westin JR, Fowler NH, et al. High complete response rates with pembrolizumab in combination with rituximab in patients with relapsed follicular lymphoma: results of an open-label, phase II study. Blood (ASH Annual Meeting Abstracts) 2017;130(Suppl):414.

31. Roussel M, Le KS, Granier C, et al. Functional characterization of PD1+TIM3+ tumor-infiltrating T cells in DLBCL and effects of PD1 or TIM3 blockade. Blood Adv 2021;5:1816-29.

32. Ahn E, Araki K, Hashimoto M, et al. Role of PD-1 during effector CD8 T cell differentiation. Proc Natl Acad Sci U S A 2018;115:4749-54.

33. Barber DL, Wherry EJ, Masopust D, et al. Restoring function in exhausted CD8 T cells during chronic viral infection. Nature 2006;439:682-7.

34. Duraiswamy J, Ibegbu CC, Masopust D, et al. Phenotype, function, and gene expression profiles of programmed death-1(hi) CD8 T cells in healthy human adults. J Immunol 2011;186:4200-12.

35. Sakuishi K, Apetoh L, Sullivan JM, Blazar BR, Kuchroo VK, Anderson AC. Targeting Tim-3 and PD-1 pathways to reverse T cell exhaustion and restore anti-tumor immunity. J Exp Med 2010;207:2187-94.

36. Utzschneider DT, Legat A, Fuertes Marraco SA, et al. T cells maintain an exhausted phenotype after antigen withdrawal and population reexpansion. Nat Immunol 2013;14:603-10.

37. Jin HT, Anderson AC, Tan WG, et al. Cooperation of Tim-3 and PD-1 in CD8 T-cell exhaustion during chronic viral infection. Proc Natl Acad Sci U S A 2010;107:14733-8.

38. Baitsch L, Baumgaertner P, Devêvre E, et al. Exhaustion of tumor-specific CD8+ T cells in metastases from melanoma patients. J Clin Invest 2011;121:2350-60.

39. Wu X, Zhang H, Xing Q, et al. PD-1+ CD8+ T cells are exhausted in tumours and functional in draining lymph nodes of colorectal cancer patients. Br J Cancer 2014;111:1391-9.

40. Kahan SM, Bakshi RK, Luther R, et al. IL-2 producing and non-producing effector CD8 T cells phenotypically and transcriptionally coalesce to form memory subsets with similar protective properties. J Immunol 2017;198:212.6.

41. Yarchoan M, Albacker LA, Hopkins AC, et al. PD-L1 expression and tumor mutational burden are independent biomarkers in most cancers. JCI Insight 2019;4:e126908.

42. Nijland M, Veenstra RN, Visser L, et al. HLA dependent immune escape mechanisms in B-cell lymphomas: implications for immune checkpoint inhibitor therapy? Oncoimmunology 2017;6:e1295202.

43. Duhen T, Duhen R, Montler R, et al. Co-expression of CD39 and CD103 identifies tumor-reactive CD8 T cells in human solid tumors. Nat Commun 2018;9:2724.

44. Ramsay AG, Clear AJ, Kelly G, et al. Follicular lymphoma cells induce T-cell immunologic synapse dysfunction that can be repaired with lenalidomide: implications for the tumor micro-environment and immunotherapy. Blood 2009;114:4713-20.

45. Ahearne MJ, Bhuller K, Hew R, Ibrahim H, Naresh K, Wagner SD. Expression of PD-1 (CD279) and FoxP3 in diffuse large B-cell lymphoma. Virchows Arch 2014;465:351-8.

46. Kwon D, Kim S, Kim PJ, et al. Clinicopathological analysis of programmed cell death 1 and programmed cell death ligand 1 expression in the tumour microenvironments of diffuse large B cell lymphomas. Histopathology 2016;68:1079-89.

47. Fang X, Xiu B, Yang Z, et al. The expression and clinical relevance of PD-1, PD-L1, and TP63 in patients with diffuse large B-cell lymphoma. Medicine (Baltimore) 2017;96:e6398.

48. Josefsson SE, Beiske K, Blaker YN, et al. TIGIT and PD-1 mark intratumoral T cells with reduced effector function in B-cell non-Hodgkin lymphoma. Cancer Immunol Res 2019;7:355-62.

49. Olsen I, Sollid LM. Pitfalls in determining the cytokine profile of human T cells. J Immunol Methods 2013;390:106-12.

Supplementary Table 1. Flow cytometry panels utilized in this study.

Panel 1	Panel 2	Panel 3
CD3	CD3	CD3
CD4	CD4	CD4
CD8	CD8	CD8
CD127	FoxP3	GzmB
CD25	GARP	Perforin
CCR6	CD45RA	cPARP
CXCR3	CCR7	-
CXCR5	CXCR5	CXCR5
PD1	PD1	PD1
HLA-DR	TIM3	TIM3
CD38	CTLA4	CTLA4
CD56	LAG3	TIGIT
CD14	CD14	-
CD33	CD33	-
CD20	CD20	CD20
CD19	PD-L1	PD-L1
Ig	Ig	-
Ig	Ig	-
CD24	PD-L2	-
CD10	IL-2	-
CD5	IFN	-
Live/dead	Live/dead	Live/dead
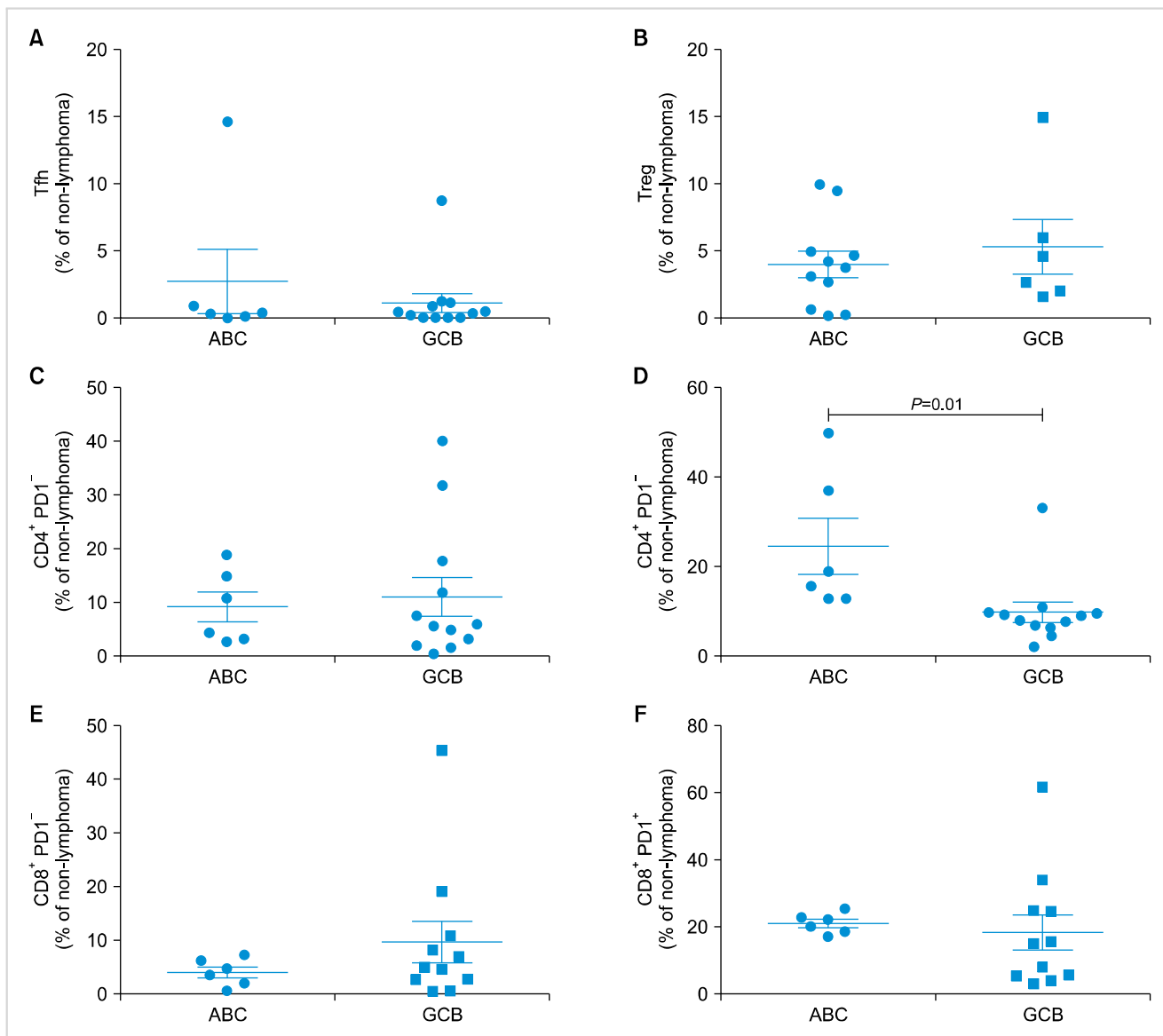
Supplementary Fig 1. Cell frequencies in DLBCL, broken down by activated B-cell (ABC) and germinal center B-cells (GCB) cell of origin. **(A)** Tfh, **(B)** Treg, **(C)** CD4$^+$ PD-1$^-$, **(D)** CD4$^+$ PD-1^{int}, **(E)** CD8$^+$ PD-1$^-$, **(F)** CD8$^+$ PD-1$^+$. Frequencies represent the proportion of cells after lymphoma cells were excluded from the analysis. GARP$^+$ Tregs, CD4$^+$ TIM3$^+$ PD1^{int} cells, and CD8$^+$ PD1$^+$ TIM3$^+$ cells are not show because only one ABC subtype sample was present in that cohort. ABC (N=6), GCB (N=11). P-values as indicated.